Efficacy of single pass UVC air treatment for the inactivation of coronavirus, MS2 coliphage and *Staphylococcus aureus* bioaerosols

William J. Snelling [a,1], Arsalan Afkhami [b,1], Hannah L. Turkington [c], Claire Carlisle [c], S. Louise Cosby [c], Jeremy W.J. Hamilton [b], Nigel G. Ternan [a], Patrick S.M. Dunlop [b,*]

[a] *Nutrition Innovation Centre for Food and Health (NICHE), School of Biomedical Sciences, University of Ulster, Coleraine, Co. Londonderry, Northern Ireland, United Kingdom*
[b] *Nanotechnology and Integrated BioEngineering Centre (NIBEC), Ulster University, Newtownabbey, Northern Ireland, United Kingdom*
[c] *Veterinary Sciences Division, Agri-Food and Biosciences Institute, Stormont, Belfast, Northern Ireland, United Kingdom*

ARTICLE INFO

ABSTRACT

There is strong evidence that SARS-CoV-2 is spread predominantly by airborne transmission, with high viral loads released into the air as respiratory droplets and aerosols from the infected subject. The spread and persistence of SARS-CoV-2 in diverse indoor environments reinforces the urgent need to supplement distancing and PPE based approaches with effective engineering measures for microbial decontamination – thereby addressing the significant risk posed by aerosols. We hypothesized that a portable, single-pass UVC air treatment device (air flow 1254 L/min) could effectively inactivate bioaerosols containing bacterial and viral indicator organisms, and coronavirus without reliance on filtration technology, at reasonable scale. Robust experiments demonstrated UVC dose dependent inactivation of *Staphylococcus aureus* (UV rate constant (k) = 0.098 m^2/J) and bacteriophage MS2, with up to 6-log MS2 reduction achieved in a single pass through the system (k = 0.119 m^2/J). The inclusion of a PTFE diffuse reflector increased the effective UVC dose by up to 34% in comparison to a standard Al foil reflector (with identical lamp output), resulting in significant additional pathogen inactivation (1-log *S. aureus* and MS2, p < 0.001). Complete inactivation of bovine coronavirus bioaerosols was demonstrated through tissue culture infectivity (2.4-log reduction) and RT-qPCR analysis – confirming single pass UVC treatment to effectively deactivate coronavirus to the limit of detection of the culture-based method. Scenario-based modelling was used to investigate the reduction in risk of airborne person-to-person transmission based upon a single infected subject within the small room. Use of the system providing 5 air changes per hour was shown to significantly reduce airborne viral load and maintain low numbers of RNA copies when the infected subject remained in the room, reducing the risk of airborne pathogen transmission to other room users. We conclude that the application of single-pass UVC systems (without reliance on HEPA filtration) could play a critical role in reducing the risk of airborne pathogen transfer, including SARS-CoV2, in locations where adequate fresh air ventilation cannot be implemented.

---

* Corresponding author.
  E-mail address: psm.dunlop@ulster.ac.uk (P.S.M. Dunlop).
[1] Authors contributed equally as first authors.

1. Introduction

The SARS-CoV-2 (COVID-19, genus *Betacoronavirus*, subgenus *Sarbecovirus*) pandemic has caused significant morbidity, mortality and global disruption (Huang et al., 2020; Wu, Wu, et al., 2020). In response governments have implemented a series of measures under emergency powers including mandatory lockdowns, closing of non-essential businesses, the requirement of wearing face coverings in public buildings, and social distancing, together with technical measures, including track and trace systems – but change is afoot with society now reopening. As the pandemic has progressed airborne transmission is now widely considered to be the main mode of transmission of SARS-CoV-2 (World Health Organisation (WHO), 2021; Greenhalgh et al., 2021; Nannu Shankar et al., 2022). People suffering from COVID release SARS CoV-2 particles within droplets when they exhale (e.g., breathing, speaking, singing, exercise, coughing, sneezing) and as such the risk of spread and persistence of SARS-CoV-2 in diverse indoor environments, including healthcare communities (Zhou et al. 2021), educational establishments, residential areas, working spaces, retail, travel, hospitality and recreational areas, underlines the urgent need for the development of effective decontamination approaches which do not rely solely on individual action (Tang et al., 2021; Wu, Zhao, et al., 2020; Lancet, 2020). Given evidence of the stability of SARS-CoV-2 aerosols with high levels of infectivity for at least 3 h (van Doremalen et al., 2020), effective engineering controls could play an important role to reduce the level of biological contaminants within indoor air as part of the strategy to permit safe access to indoor spaces (Lewis, 2021; Zhang et al., 2011) (but they should not be considered a magic bullet). Appropriate building engineering controls include effective fresh air ventilation, possibly enhanced by particle filtration and/or air disinfection, with care taken to reduce 'stale' air recirculation and prevent overcrowding (Lewis, 2021), however, there are many environments where sufficient ventilation cannot be supplied and invariably thermal comfort in many settings needs also to be addressed.

Various chemical and physical based technologies could be adopted to remove coronaviruses from air, as recently reviewed by Berry et al. (2022), with UV irradiation commonly implemented due to its well understood and highly efficacious mode of action, coupled to chemical-free and low-cost production technologies (Chiappa et al., 2021; Nardell, 2021). In terms of general pathogen removal, ultraviolet germicidal irradiation (UVGI) has a multi-modal mechanism of inactivation which includes damage to nucleic acids (Rastogi et al., 2010; Beck et al., 2015), proteins (Eischeid & Linden, 2011), and/or internal production of oxygen radicals (Gerchman et al., 2019). Whilst the mechanism of inactivation depends on the UV wavelength(s) applied (UVC 200–280 nm; UVB 280–315 nm; UVA (315–380 nm), UVC with wavelength 254 nm is predominantly employed for effective, fast germicidal applications - based upon the peak DNA absorption at 260 nm (Eischeid & Linden, 2011).

Retrofitting large air treatment devices into existing buildings is likely to be prohibitively expensive (Megahed & Ghoneim, 2020) and in many cases unnecessary if other interventions are deemed appropriate, however, significant transmission risk remains in highly populated indoor spaces in which adequate ventilation cannot be ensured (Morawska et al., 2020). The ability to deploy an effective, self-contained, room-based air disinfection unit capable of high throughput air exchange of between 4 and 10 air changes per hour (ACH), could be an important cost-effective tool to reduce the risk of airborne pathogen transfer, thereby aiding in the development of a safer working environment for small, medium and large spaces (SAGE, 2021; Elias & Bar-Yam, 2020). Recent studies have confirmed that as little as 2-ACH can be more effective than mask wearing within indoor spaces (Shah et al., 2021). Modelling the effect of air sterilisation systems to reduce viral load can aid understanding of the potential reduction in risk of person-to-person transmission in poorly ventilated indoor spaces. The risk of airborne cross-infection has been investigated via mass balance models to determine the role of transient effects and the role purging room air during breaks (Melikov et al., 2020), with Jones et al. (2021) developing a relative exposure index considering factors that increase the likelihood of far field (>2 m) exposure to SARS-CoV-2. Coupled to robust testing of system efficacy, an understanding of the reduction in the risk of person-to-person transmission through introduction of air sterilisation systems, could play an important role in demonstrating the impact and value of air sterilisation in poorly ventilated spaces.

Whilst there has been significant research into UVGI technologies for disinfection of air over many years (as reviewed by Reed, 2010) the majority of commercial UVGI system lack independent data to support the efficacy of the device, often place significant reliance on pre-HEPA filtration and thereby do not address the primary technical challenge of delivery of sufficient UV dose to large volumes of air (Cutler & Zimmerman, 2011). Recent academic interest has been focused on small scale, laboratory-based experiments demonstrating efficacy against liquid-based pathogens placed on surfaces, including SARS-CoV-2 (Inagaki et al., 2020), or examination of novel UV sources which require significant exposure times – without attempt to consider scale-up or application of treatment to indoor spaces with realistic timeframes. For example, Buonanno et al. (2020) demonstrated the effectiveness of 222-nm (far-UVC) towards viral airborne influenza virus, concluding that ~25 min exposure would be required to attain 99.9% inactivation, and whilst this is promising with respect to human safety, the current cost of the technology and energy delivered prevent practical application. The application of UVC LED technology has also been reported to be effective against coronaviruses in liquid suspension tests however, again, cost-effective commercial application is challenging (Gerchman et al., 2020).

UVGI microbial inactivation kinetics are directly related to the total UV energy absorbed, with engineering approaches often focused on understanding system UV dose (a function of irradiance and exposure time). To reduce power input, approaches to enhance UV dose through implementation of reflective surfaces on the chamber walls has gained attention (Ryan et al., 2010; Thatcher & Adams, 2021). A wide range of materials have been examined for this purpose, including polished metals (specular reflectors) and metal oxide films, with a range of specifically modified polymers now becoming available, including sintered polytetrafluoroethylene (PTFE) for which >98% diffuse (or Lambertian) reflectivity in the UV range has been reported (Janecek, 2012).

Seminal work by Jensen (1964, 1967), Tseng and Li (2005) and Walker and Ko (2007) reported the inactivation of aerosolised coxsackie, influenza, Sindbis, and vaccinia viruses, a range of bacteriophages and MS2, and adenovirus and murine coronavirus, respectively, demonstrating the effect of UV dose on the inactivation kinetics. However, only a small number of studies focus on developing understanding of the properties and application of reflectors for UVC air disinfection. Ryan et al. (2010) discussed UVGI treatment of *Bacillus subtilis* and *Mycobacterium parafortuitum*, demonstrating an enhanced fluence rate – by a factor of 1.6 – upon inclusion of a proprietary high-reflectance surface coating (>90% reflectance at 254 nm) over bare uncoated aluminium. Thatcher and Adams (2021) recently modelled the effects of inclusion of PTFE reflective materials in an LED-based air treatment duct and conducted small scale experiments demonstrating a 3-log inactivation of *Staphylococcus aureus* in a $20 \times 20 \times 120$ mm prototype duct under low flow conditions (0–70 L/min). To further understand the effects of fluence, reflectors and geometry within small footprint LED based UVC systems, computational analysis was undertaken by Lombini et al. (2021) in which simulations suggested efficacy against SARS-CoV-2 in high air flux systems.

Given the paucity of published literature relating to potential efficacy of UVC air treatment to aid in reduction of person-to-person transmission of SARS-CoV-2, the aim of this work was to investigate the efficacy of a high velocity, single pass system to deactivate relevant model pathogens (MS2, *Staphylococcus aureus*, bovine coronavirus) – thereby negating the need for recirculation of air multiple times through the device and/or reliance on HEPA filtration. To aid with translation of the lab-based data to real world environments, scenario-based modelling was implemented within a small indoor space to investigate the potential to reduce the risk of person-to-person transmission.

2. Materials and methods

2.1. UVC device specification

A UVC air treatment device was developed in collaboration with Ilimex (Ballycastle, Co. Antrim, UK) comprising a stainless-steel housing (1 mm material thickness) and baffles to create three consecutive UVC exposure chambers (1000 (l) × 68 (w) × 97 (h) mm) resulting in a treatment pathlength of 2.775 m and chamber volume of 0.018 m^3 (Fig. 1). Air passed from chamber 1 to 2 (and 2 to 3) via a 50 × 86 mm window in the respective baffle plate. The system included 5 compact UVC lamps (Philips TUV PL-L 55 W, peak emission 254 nm), arranged in series along the length of the chamber. Independent operation permitted examination of increasing UVC output. Lamps were secured to a stainless-steel lid and when assembled the sources were maintained at a height of 90 mm (right hand lamp) and 50 mm (left hand lamp) from the floor of chambers 1, 2 and 3 (i.e. within the void through which the air passed). The lid was screwed onto the chamber walls and internally sealed via inclusion of a foam-based adhesive along the top surface of the perimeter wall and chamber baffles. A 12 V DC fan blower (Delta Electronics, BFB1212GH-AF00) was secured in place at the air inlet. A HEPA/carbon filter (Maxvac) was included after the air sampling port simply to remove dust from within the environment. The walls, floor and roof of the system were lined with either highly polished aluminium foil (Bacofoil, UK) or 2 mm thick polytetrafluorethylene (optical PTFE) foam (Porex, Virtek PMR20). Air speed was measured using a vane anemometer (Infurider, YF-866B) at the fan exit, the window between chamber 1 and 2, and at the exit port, with the average volumetric flow rate calculated to be 1254 L/min (0.021 m^3/ s) – the size of the anemometer ensured measurement of air flow at the boundary layer. UVC exposure time was therefore calculated to be 0.29 s in chamber 1, 0.57 s chamber 1 & 2, with a maximum exposure time of 0.86 s (chamber 1, 2 & 3).
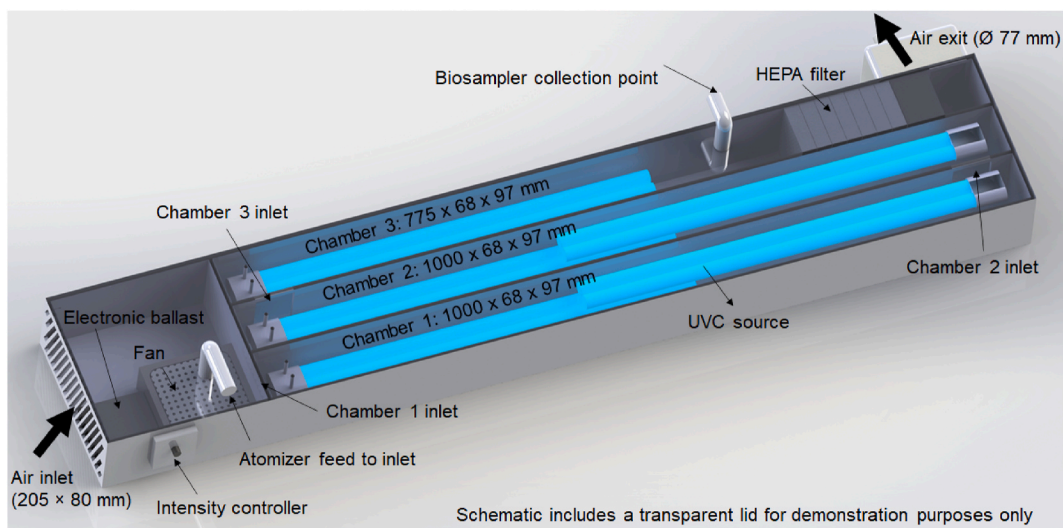

Fig. 1. Schematic representation of the UVC air treatment device.

2.2. Quantification of UVC dose

UVC intensity was measured using a radiometer (Linshang, LS125) with a 254-nm sensor (Linshang, UVC-X0, radiant power measured between 230 and 280 nm). UVC lamps were permitted 30 min to warm up prior to any experimentation. To profile UVC irradiance along length of the chamber, the radiometer sensor was placed in the centre of the floor of chamber 1 (sensor window at 2.5 cm from the wall) with facial intensity recorded at 2 cm intervals along the entire length of the chamber. Measurements were recorded in duplicate with the chamber lined with aluminium foil or PTFE reflector, and during irradiation with 1, then 2 UVC lamps. The effect of reflector material on measured UVC dose was evaluated, where dose is defined as the product of exposure time and UV irradiance between 230 and 280 nm, in-keeping with Bolton's definition 'the total radiant power incident from all upward directions on an infinitesimal element of surface of area δA, containing the point under consideration divided by δA' (Bolton & Linden, 2003). The first-order decay rate constant (k) was calculated using (Kowalski, 2009):

$$S = e^{-kD} \tag{1}$$

where, S = Survival, fractional (i.e. the number of viable microorganisms downstream of UV-C exposure/number of viable microorganisms upstream of UV-C); k = UV rate constant, m^2/J; and D = UV exposure dose (fluence), J/m^2.

2.3. Chemicals, glassware and media

All glassware was sterilised by soaking overnight in 1% Virkon (Antec, UK) and steam sterilised in an autoclave at 121 °C for 15 min prior to use. All culture media (Oxoid, UK) was prepared as per the manufacturer's instructions. Phosphate buffered saline (Oxoid, UK) was prepared in deionised water and steam sterilised in an autoclave prior to use.

2.4. Preparation and enumeration of microorganisms

Staphylococcus aureus (ATCC 29213) and *Escherichia coli* (ATCC 15597) were cultured at 37 °C using Tryptone Soya Broth (TSB) and Tryptone Soya Agar (TSA). The bacterial coliphage MS2 (ATCC 15597-B1) was grown with strain *E. coli* as the host in TSB and harvested using chloroform and filtration (0.2 μM) as described by Bonilla et al. (2016) to a confirmed titre of 1.3×10^{12} PFU/mL. All bacterial and MS2 stocks were stored at -80 °C in glycerol stocks.

In preparation for treatment experiments, *S. aureus* was inoculated into 10 mL of TSB and grown for 18 h at 37 °C at 200 rpm in 50 mL sterile centrifuge tubes (Merck, Dorset UK). Consistent amounts of *S. aureus* cells were obtained from overnight cultures (3.2×10^9 to 3.3×10^9 CFU/mL). A frozen aliquot of MS2 stock was thawed on ice with a reproducible titre of between 1.30×10^{12} to 1.64×10^{12} PFU/mL. All MS2 phage samples were enumerated using the soft agar (TSA) overlay (double-agar layer) method with *E. coli* strain ATCC 15597 as the host. *S. aureus* concentrations were determined using the spread plate method on TSA after culture for 24 h at 37 °C (Missiakas & Schneewind, 2013, chap. 9). Upon receipt of treated samples from the biosampler, samples were serially diluted in PBS with bacterial and MS2 viability assessed by triplicate plate count.

2.5. Growth of bovine coronavirus and titre confirmation

Bovine coronavirus (BCoV) isolate 438/06 originating from 2 to 3 month-old cattle in Italy was stored at −80 °C until cultivation. MDBK cells ATCC CCL 22 (Public Health, Salisbury, UK) were grown to 90% confluency in Minimum Essential Media (Gibco, Cambridge, UK) and infected at a multiplicity of infection of 0.001 to produce a BCoV stock. BCoV stock titre was confirmed by Median Tissue Culture Infectious Dose (TCID50) in MDBK cells via serial dilution to be 10^9 TCID50/ml.

2.6. Enumeration of bovine CoV

Upon receipt of treated samples, an aliquot was prepared through a series of 10-fold dilutions (10^{-1} to 10^{-11}) in MEM media supplemented with penicillin (100 U mL^{-1}), streptomycin (100 μg mL^{-1}), non-essential amino acid solution (1x) and L-Glutamine (2 mM). In replicates of 8, 200 μL aliquots of diluted samples were added to pre-washed MDBK cells in 96-well plates and incubated at 37 °C for 7 days prior to observation of cytopathic effect via microscopy (Leica DMi1 microscope). TCID50 values were calculated using the Reed-Muench method.

2.7. Methods for PCR

RNA extraction of BCoV samples was undertaken using the QIAamp Viral RNA Mini kit (Qiagen). One-step reverse transcription real-time PCR was performed using the ViroReal Bovine Coronavirus Kit (Ingenetix) on a LightCycler® 480 II (Roche).

2.8. Bioaerosol production and air sampling

Bioaerosols were generated using a single-jet particle generating atomizer (model 9302, TSI Instruments, Buckinghamshire, UK) and directed into the air intake of the air treatment system (Fig. 1), whereby the atomiser nozzle was inserted through the top surface of

the stainless-steel casing via a 10 mm diameter hole to a depth of 15 mm below the surface, delivering bioaerosol from the 3 mm internal diameter nozzle tip towards the system fan. Air samples were collected using a biosampler, (BioLite + Pump, SKC Limited, Dorset, UK), with air sampled at the end of the UVC chamber, prior to HEPA filter. The sampling probe consisted of a 10 mm internal diameter silicone tube extended into the middle of the chamber (50 mm below the top surface of the treatment system). The biosampler withdrew air samples at a fixed rate of 12.5 L/min with sonic flow delivering all airborne particles into 20 mL of sterile PBS.

All equipment was maintained in a vented and extracted air handling cabinet, based upon the methods reported by Turgeon et al. (2014). The atomiser delivering microbial suspension droplet-based vapour at a flow rate of 12 mL per hour, with a number mean particle diameter of approx. 0.8–1.5 μm (at 25 psi) – representing small, expired droplets from human subjects (expired droplet size is reported to be within the range of 0.1 μm–1 mm, with greater than 5 μm often considered the 'large' droplets that fall with gravity (Blocken et al., 2021; Mittal et al., 2020)). For each treatment experiment, 1 mL of MS2, or *S. aureus*, was diluted 1/100 in sterile PBS and transferred to the atomiser reservoir which was kept at room temperature for the duration of all treatment runs. For assessment of BCoV, viral particles from stock were diluted 1/10 in MEM media.

Air sampling was conducted for periods of 30 min (sampling 375 L of air per experiment), followed by serial dilution of the biosampler vial contents in sterile PBS and enumeration of microbes as described above. Air temperature and relative humidity were not specifically controlled within the air handling cabinet, but frequently measured at $50 \pm 2\%$ RH and 18 ± 2 °C (typical indoor air conditions). During UVC treatments the temperature of the device was measured at 30 min intervals with an infrared thermometer (MM-IT01, Max Measure, UK), and at no time did the surface temperature rise above 40 °C.

2.9. Control experiments and statistical analysis

Control experiments were performed to determine the effects of atomisation on microbial viability, using samples removed from the atomiser reservoir and samples of atomised microbes collected by condensation into a sterile Falcon tube. Baseline 'air only' experiments (0 mJ/cm^2 UVC) were conducted with passage of microbes through the device assessed in quadruplicate. Each UVC exposure experiment was repeated in duplicate, with replicate experimental runs conducted with new pathogen stock. Data points from culture-based enumeration methods and repeated experimental analysis are reported as mean values. A two-tailed *t*-test was used to assess significance of the inclusion of the PTFE liner.

2.10. Scenario based risk modelling

The model developed by Jones et al. (2021) for estimation of the relative risk of exposure to SARS-CoV-2 was adopted to investigate the practical application of the prototype device to remove COVID-19 RNA copies in an appropriate small room (e.g. medical examination room, small office etc. of 15 m^3). We consider that the space has no fresh air ventilation, with the UVC prototype implementing 5 air changes per hour (ACH) (SAGE, 2021) with the lowest UVC dose (the system with a single lamp would have the footprint of a shoe box). The scenario considered a single infector (an adult male) sitting for 5 h shedding virus at a constant rate ($G = 29.2$ RNA copies/s, as described in detail by Jones et al. (2021)). The air within the room was assumed to be well-mixed with virus removal due to only biological decay and UVC inactivation within the treatment system. The rate of change in the number of viral RNA copies (*n*) in the space at time *t* (s) was expressed as:

$$\frac{dn}{dt} = G - n(t)\varphi \tag{2}$$

where φ (s^{-1}) is the total removal rate, calculated as the sum of biological decay ($\lambda = 0.000148$ s^{-1}), surface deposition ($\gamma = 0.000143$ s^{-1}), and the ventilation removal rate of the device based on the 2.4-log inactivation of bovine CoV achieved with the minimal UVC dose of the prototype (5 mJ/cm^2), $\psi = 0.00139$ s^{-1}.

The effect of the system on airborne viral load was investigated for a period of 5 h through three scenarios in which the infected subject remained seated in the room: (i) the UVC device turned off; (ii) the device turned on as the subject enters the room at time zero; (iii) subject entering at time zero, with the device turned on at $t = 2.5$ h. The *Relative Exposure Index* (REI) approach of Jones et al. (2021) was adopted to determine the impact of system introduction with one room occupant exposed to the single infected subject over a 5 h period (respiratory activity 75% breathing: 25% talking, no natural ventilation); given these constraints, the rate of reduction in the number of RNA copies equals the rate of change in the REI.

3. Results & discussion

3.1. Assessment of UV fluence rate and UV dose

Fig. 2 details the irradiance profile at the chamber floor as a function of Al or PTFE reflector during exposure to single or dual lamps (sensor positioned at a height of 15 mm from the lamp). Lower output is measured at either end of the fluorescent tube, due to a reduction in direct irradiation. The intensity was observed to vary along the length of the chamber, rising to a peak in the middle of the chamber resulting from the short overlap of sources in the dual lamp system. The fluctuation in intensity with the polished Al foil liner, in comparison to the smooth response of the PTFE, results from minor creasing during manual placement of the Al liner and the specular and diffuse reflective property of the materials, respectively.
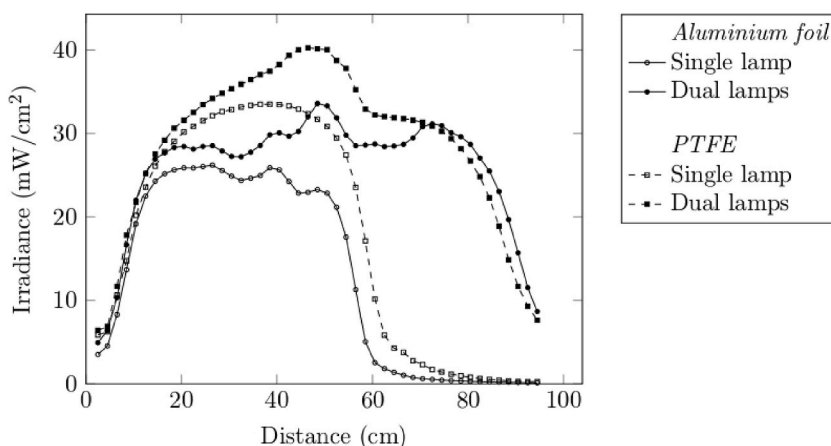
Fig. 2. Irradiance profile within the air treatment chamber demonstrating a significant enhancement in UVC irradiance upon inclusion of PTFE liner in comparison to Al foil.

Table 1
Calculated UV dose relative to number of lamps and reflector material.

Lamps	Active chambers	Exposure time (s)	UV dose Al (mJ/cm^2)	UV dose PTFE (mJ/cm^2)
1	1	0.29	3.72	5.00
2	1	0.29	7.42	8.27
3	1 & 2	0.59	11.14	13.27
4	1 & 2	0.59	14.84	16.54
5	1 & 2 & 3	0.86	18.56	21.54

Increased facial intensity was observed with the PTFE liner vs the Al foil, resulting from additional reflectivity at 254 nm for PTFE (>97%) in comparison to Al (~75%) primarily due to the diffuse property of the sintered PTFE (Quill et al., 2016). Analysis of the cumulative energy from a single lamp demonstrated a 34% increase upon inclusion of the PTFE chamber liner (vs Al foil), with an 11% increase observed with dual lamp. Commercial literature often describes a greater increase in reflected energy through inclusion of PTFE materials in comparison to metallic reflectors (Porex Filtration Group, 2021; de Sternberg Stojalowski & Fairfoull, 2021), though measurements are made using low-power sources and at distances of up to 1.5 m from the source via qualitative sensors, thus preventing a direct comparison.

Cumulative irradiance divided by the sampled area (base of chamber 1) permitted calculation of the area-weighted average facial intensity (mW/cm^2), which is often considered equivalent to the minimal fluence rate. The product of exposure time and fluence rate dictated the fluence, the UV dose (mJ/cm^2), as reported in Table 1.

The challenges of accurate measurement and modelling of UV dose and the associated comparison to microbial inactivation have been raised by several authors. Ryan et al. (2010) determined the fluence rate via actinometry and a radiometric approach yielding reasonable agreement (12% difference) describing how classical fluence models do not accurately reflect complex system geometries nor consider UV reflection or air flow profiles. To aid in reactor development, Retamar et al. (2019) proposed a radiation field model for an annular reactor and demonstrated validity through radiometric measurement and experimentation. Given the debate, the work in this manuscript follows recommendations by Lombini et al. (2021), and references within, who draw particular attention to the necessity of experimental validation of microbial inactivation rather than reliance on prediction from energy/dose measurements.

3.2. Bioaerosol characterization

To ensure a standardised approach to determination of microbial inactivation during treatment, regular pre-assessments and controls were routinely conducted. Enumeration of diluted stock MS2 from the atomiser reservoir at start and end of experimental sessions confirmed viability with a concentration of 10.1 log ±10% observed throughout long (8 h) experimental runs. Enumeration of atomised MS2 samples collected directly at the atomiser exit via condensation into a Falcon tube, consistently yielded concentrations matching that of the atomiser reservoir demonstrating the coliphage to be resilient to the atomisation process. Air sampled directly from the atomiser exit confirmed passage and collation of MS2 in the biosampler reservoir without loss viability. Similar findings were reported by Turgeon et al. (2014), who demonstrated the stability of MS2 upon atomisation and biosampling with a range of equipment and supporting media.

Likewise, with *S. aureus*, atomisation alone did not affect viability with 7.46 log ±10% quantified per mL. Processing atomised *S. aureus* directly into the biosampler resulted in a 0.88 ± 0.12 log reduction due to physical/mechanical inactivation, demonstrating the gentle nature of the biosampler sonic flow technology towards bacteria.

3.3. UVC inactivation of aerosolised MS2 and S. aureus

Tables 2 and 3 summarise MS2 and *S. aureus* inactivation, respectively. Baseline control experiments in the absence of UV (0 mJ/cm^2), termed 'air only', were undertaken to permit direct comparison of the effect of increasing UV dose. Following 30 min 'air only' treatment, the MS2 titre at the sampling port was determined to be 6.48 $\pm$ 0.17 log PFU/mL; in-keeping with the expected dilution factor and therefore demonstrating capacity within the experimental set-up and methods to assess up to 6-log inactivation resulting solely from the effects of UV treatment. Passage of aerosolised *S. aureus* through the treatment device with 'air only' resulted in recovery of 4.70 $\pm$ 0.16 log CFU/mL, representing the maximum inactivation quantifiable with UV treatment.

Inactivation experiments were performed with increasing number of UV sources, demonstrating a dose dependent response (Tables 2 and 3 and Fig. 3). Complete inactivation (4.7-log) of *S. aureus* was achieved with lower energy upon inclusion of the PTFE liner (1.25 log difference when compared to Al foil; p < 0.001) demonstrating the practical effect of the enhanced diffuse reflectivity of the PTFE liner. Increased UVC dose was required to reach complete inactivation of MS2, however a 6.48-log reduction was confirmed. The increased reflectivity of the PTFE liner again demonstrated a practical effect with approx. 1-log additional inactivation (p < 0.01) observed when compared to Al wall liners with equivalent lamp output. Fig. 3 shows the UV survival curve for MS2 and *S. aureus*, in which the D90 for MS2 (dose required for 90% MS2 inactivation) equals 20 J/m^2 with an inactivation rate constant (k) of 0.119 m^2/J,

Table 2
Reduction in number of coliphage MS2 with respect to UVC dose and reflector material.

Reflective surface	UV dose (mJ/cm^2)	Mean log count (PFU/mL) $\pm$ SD	Log reduction
–	0	6.48 $\pm$ 0.17	–
Al foil	3.72	4.43 $\pm$ 0.05	2.05
PTFE	5.00	3.16 $\pm$ 0.11	3.32
Al foil	7.42	3.51 $\pm$ 0.10	2.97
PTFE	8.27	2.32 $\pm$ 0.09	4.16
Al foil	11.14	0	6.48
PTFE	13.27	0	6.48
Al foil	14.84	0	6.48
PTFE	16.54	0	6.48
Al foil	18.56	0	6.48
PTFE	21.54	0	6.48

Table 3
Reduction in number of *S. aureus* with respect to UVC dose and reflector material.

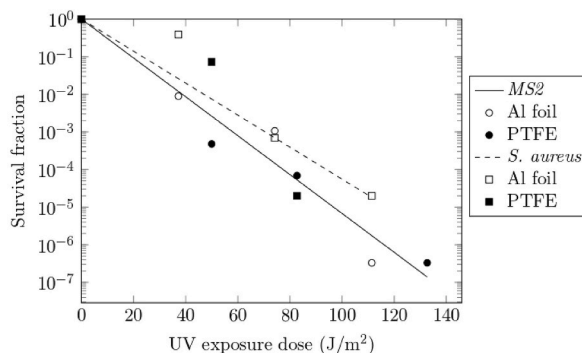| Reflective surface	UV dose (mJ/cm^2)	Mean log count (CFU/mL) $\pm$ SD	Log reduction
–	0	4.70 $\pm$ 0.16	–
Al foil	3.72	4.29 $\pm$ 0.01	0.41
PTFE	5.00	3.56 $\pm$ 0.03	1.14
Al foil	7.42	1.54 $\pm$ 0.34	3.16
PTFE	8.27	0	4.70
Al foil	11.14	0	4.70
PTFE	13.27	0	4.70
Al foil	14.84	0	4.70
PTFE	16.54	0	4.70
Al foil	18.56	0	4.70
PTFE	21.54	0	4.70

Fig. 3. Survival curve for MS2 and *S. aureus* bioaerosols under UVC exposure. Trendlines represent curve fits to the exponential decay equation (Eq (1)).

both figures lying within the range reported by Tseng and Li (2005) and Walker and Ko (2007); and a D90 and *k* for *S. aureus* equal to 23 J/m² and 0.098 m²/J respectively.

We report large velocity UV sterilisation (1254 L/min) attaining 6-log inactivation of MS2 via single pass treatment, without reliance on HEPA filtration. Previous work in this area has been primarily based on laboratory systems with low flow rates (e.g. 0.2–4 L/min (Ryan et al., 2010), 33 L/min (Retamar et al., 2019), 60 L/min (Walker & Ko, 2007) and up to 120 L/min (Thatcher & Adams, 2021) where multiple passes and very small air change rates prevent practical application to the challenge presented by airborne viral pathogens within indoor spaces.

3.4. Inactivation of bovine CoV

Bovine CoV was used as a surrogate for SARS-CoV2 with experiments conducted with air treatment system walls lined with PTFE. BCoV titres were stable in MEM media (±10%) for up to 3 h during storage in the atomiser reservoir, with fresh stock prepared if required (TCID50/mL = 6.5 log). Atomisation did not significantly reduce the titre. Optical microscopy images of the tissue culture infectivity assay are shown in Fig. 4. The qualitative effect of high BCoV infectivity upon with the confluent growth of host cells (Fig. 4A), is evident in Fig. 4B where the cytopathic effect can be observed by characteristically rounded and floating 'inactivated' host cells. Fig. 4D represents the effects of UVC air treatment of BCoV, in which the confluent growth demonstrates no infectivity from the applied viral particles – the UVC treatment has completely inactivated the bovine coronavirus. The cytopathic effect was quantified through the TCID50 method, with data presented in Table 4. Passage through the air treatment system in the absence of UVC resulted in reduction of titre to 2.4 log ±0.14. Based upon the MS2 dilution though the system, the 4-log BCoV reduction factor represents an additional 1-log reduction, resulting from physical/mechanical stress and/or desiccation effects on this more susceptible pathogen. Complete inactivation (2.4-log being the maximum attainable reduction with the viability assay used) was observed following passage through the system with the lowest UVC dose vs the 'air only' controls (0 mJ/cm²). RT-qPCR demonstrated levels of BCoV RNA remained equivalent both pre- and post- UVC treatments. Consequently, we conclude that while the viral particles physically remained in the air, we demonstrate UVC treatment renders the particles non-infectious. A similar molecular based assessment mechanism was
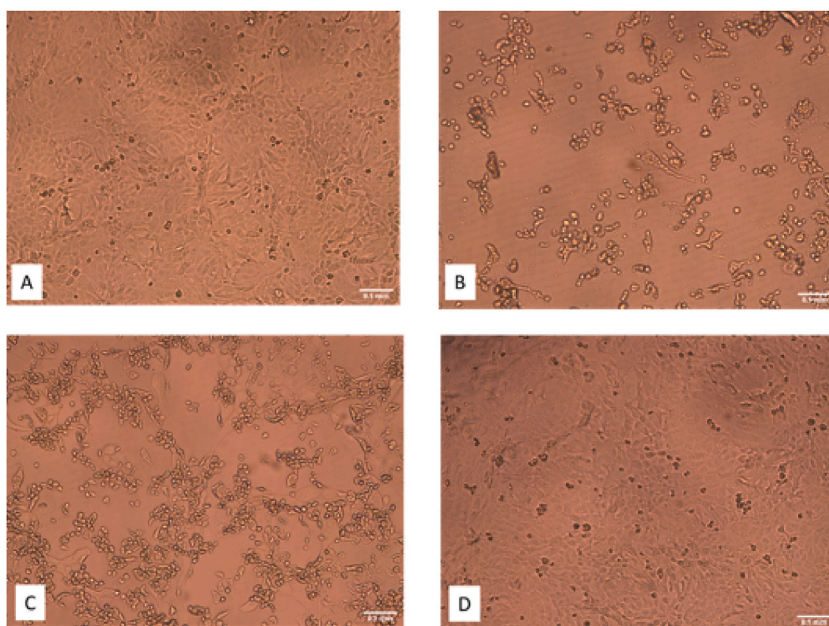
Fig. 4. Example optical microscopy images of the BCoV tissue infectivity assay (×10 magnification), A) Negative control; B) Positive control; C) Air only (0 mJ/cm²), note the mix of viable cells and floating inactivated cells; D) UVC treated sample (5.0 mJ/cm²), no evidence of cytopathic effect due to BCoV inactivation. (Scale bar = 0.1 mm)

Table 4
Viability assessment of bovine CoV following UVC treatment.

UV dose (mJ/cm²)	Mean TCID50/mL	Log reduction	Mean qRT-PCR Ct ± SD
0	2.40 ± 0.14	–	
5.00	0.00	2.40	29.80 ± 0.99
8.27	0.00	2.40	25.20 ± 7.35
13.27	0.00	2.40	30.65 ± 0.07

reported by Qiao et al. (2021) during UVC disinfection of bioaerosols, with systematic losses within the duct system similarly not observed.

There is a growing interest in methods to reduce the risk of airborne transmission of viral pathogens on farms (Arruda et al., 2019), and to the best of our knowledge this is the first report of effective UVC inactivation of airborne bovine coronavirus, a pathogen which is associated with calfhood diarrhoea (Mebus et al., 1972) and implicated as a contributor in the development of bovine respiratory disease complex (Ng et al., 2015).

Walker and Ko (2007) conducted research on the UV susceptibility of MS2 and murine hepatitis virus (MHV) coronavirus as viral aerosols exposed to a range of UV doses (source output at 254 nm), determining that UVC treatment of coronavirus aerosols required 7–10 times less energy (UVC dose) than MS2, approximately 2.7 mJ/cm^2 for 1-log reduction of MHV (D90). Following the 2009 H1N1 influenza (swine flu) pandemic, McDevitt et al. (2012) demonstrated susceptibility of H1N1 to UVC doses ranging from 4 to 12 J/m^2 showcasing the potential for effective upper-room UVC installations to prevent airborne transmission of influenza. During the more recent pandemic, Biasin et al. (2021) reported 3-log inactivation of SARS-CoV-2 with a UVC dose of 3.7 mJ/cm^2 but highlighted the variation in literature-reported doses ranging from 3 to 1000 mJ/cm^2. At approximately the same time, Qiao et al. (2021) reported inactivation of porcine respiratory coronavirus in a duct based, single pass UVC system. Using culture-based viability assays they measured inactivation in excess of 2.2-log at a flow rate of 2439 L min^{-1} (13.9 mJ/cm^2) and 3.7-log at 684 L min^{-1} (49.6 mJ/cm^2). The authors also note the challenge of developing high viral load bioaerosols and the limitations presented by low sensitivity culture-based infectivity assays – as such UVC inactivation of coronaviruses could indeed be greater than that measured and reported in these studies. The 3-log coronavirus deactivation at the lowest dose attainable in this work (a minimum of 5.0 mJ/cm^2 with a single lamp and PTFE liner) is therefore well within the expected effective dose with findings concurring with those reported in the above studies.

3.5. Modelling implementation in real-world scenarios

Fig. 5 shows the number of viral RNA copies, $n(t)$, over time for three indoor room-based scenarios, where the prototype system is operated at its minimum UVC dose. Without the device (A), $n(t)$ continuously rises during the 5 h period, whereas with the presence of the device in the room upon arrival of the infected subject (B), a low-level steady state was quickly achieved (0.49 h to reach 95% of the steady state number) and maintained (after 5 h the steady state number of RNA copies remained 82.57% lower than in the absence of a device). In the scenario in which the device was turned on 2.5 h after arrival of the infected subject (C), the model predicts the number of RNA copies to be quickly reduced to that of the 95% steady state (within 0.72 h) and constantly maintained at this low level. The introduction of the system over the 5 h period reduced the relative exposure index (REI) by 81.9% demonstrating a significant reduction of the risk of airborne person-to-person transmission.
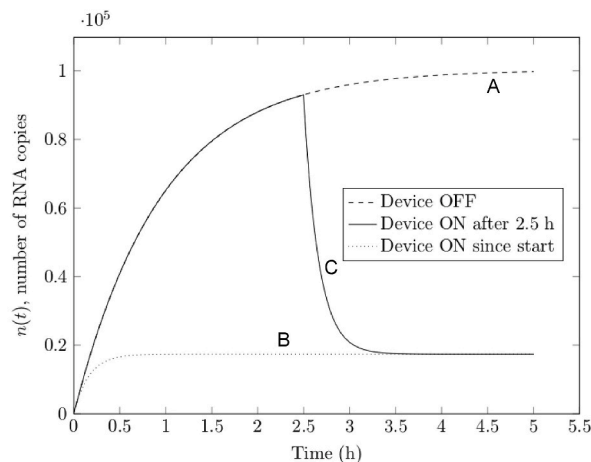

Fig. 5. Modelled effect of UVC prototype to reduce aerosolised SARS-CoV-2 from a single infector in a 15 m^3 room. A: Device turned off; B: Device switched on at T0; C) Device switched on at T 2.5 h (Modelling conditions: Well-mixed air, shedding rate of 29.2 RNA copies/s, removal due to biological decay, natural particle deposition and UVC treatment, UV dose of 5 mJ/cm^2, fan flow rate of 1254 L/min)

4. Conclusion

We demonstrate that single pass UVC air treatment (1254 L/min) can effectively inactivate MS2 (6-log reduction), *S. aureus* (4.7-log reduction) and bovine coronavirus (2.4-log reduction) with a relatively small footprint prototype (to the limits of detection of the assays employed). Inclusion of a PTFE wall liner generated increased UVC reflection permitting additional inactivation of *S. aureus* and MS2 (approx. 1-log) vs a standard Al reflector, demonstrating the potential for reactor engineering to play a role in enhancing UV dose to further reduce the system footprint. Modelling demonstrated the small prototype to be effective at the lowest UV dose within an indoor setting, where a significant reduction in viral DNA copies was quickly achieved and maintained – reducing the relative risk of airborne SARS-CoV-2 transmission from the infected subject. Although the parallel arrangement of the lamps to the air flow provides effective exposure of pathogens to the photons, further optimisation of lamp power and position relative to the reflective surface could be undertaken with the multi-source configuration in conjunction with increasing air flow. Future studies will also be directed towards reduction in device footprint and energy consumption, and validation of the modelling in simulated and real-world settings.

Author contributions

William Snelling: Methodology, Investigation, Writing - Original draft preparation. Arsalan Afkhami: Investigation, Formal analysis, Visualization, Writing - Review & Editing, Hannah Turkington: Investigation, Formal analysis, Visualization, Writing - Review & Editing, Claire Carlisle: Investigation, Writing - Review & Editing, Louise Cosby: Supervision, Writing - Review & Editing, Jeremy Hamilton: Investigation, Formal analysis, Writing - Review & Editing, Nigel Ternan: Supervision, Conceptualization, Investigation, Writing - Review & Editing, Patrick Dunlop: Supervision, Conceptualization, Investigation, Formal analysis, Writing - Review & Editing.

Declaration of competing interest

The authors declare that they have no known competing financial interests or personal relationships that could have appeared to influence the work reported in this paper.

Acknowledgements

References

Arruda, A. G., Tousignant, S., Sanhueza, J., Vilalta, C., Poljak, Z., Torremorell, M., Alonso, C., & Corzo, C. A. (2019). Aerosol detection and transmission of porcine reproductive and respiratory syndrome virus (PRRSV): What is the evidence, and what are the knowledge gaps? *Viruses, 11*(8). https://doi.org/10.3390/v11080712. Article 712.

Beck, S. E., Rodriguez, R. A., Hawkins, M. A., Hargy, T. M., Larason, T. C., & Linden, K. G. (2015). Comparison of UV-induced inactivation and RNA damage in MS2 phage across the germicidal UV spectrum. *Applied and Environmental Microbiology, 82*(5), 1468–1474. https://doi.org/10.1128/AEM.02773-15

Berry, G., Parsons, A., Morgan, M., Rickert, J., & Cho, H. (2022). A review of methods to reduce the probability of the airborne spread of COVID-19 in ventilation systems and enclosed spaces. *Environmental Research, 203*. https://doi.org/10.1016/j.envres.2021.111765. Article 111765.

Biasin, M., Bianco, A., Pareschi, G., Cavalleri, A., Cavatorta, C., Fenizia, C., Galli, P., Lessio, L., Lualdi, M., Tombetti, E., Ambrosi, A., Redaelli, E., Saulle, I., Trabattoni, D., Zanutta, A., & Clerici, M. (2021). UV-C irradiation is highly effective in inactivating SARS-CoV-2 replication. *Scientific Reports, 11*(1). https://doi.org/10.1038/s41598-021-85425-w. Article 6260.

Blocken, B., van Druenen, T., Ricci, A., Kang, L., van Hooff, T., Qin, P., Xia, L., Ruiz, C. A., Arts, J. H., Diepens, J., Maas, G. A., Gillmeier, S. G., Vos, S. B., & Brombacher, A. C. (2021). Ventilation and air cleaning to limit aerosol particle concentrations in a gym during the COVID-19 pandemic. *Building and Environment, 193*. https://doi.org/10.1016/j.buildenv.2021.107659. Article 107659.

Bolton, J. R., & Linden, K. G. (2003). Standardization of methods for fluence (UV dose) determination in bench-scale UV experiments. *Journal of Environmental Engineering, 129*(3), 209–215. https://doi.org/10.1061/(ASCE)0733-9372(2003)129:3(209)

Bonilla, N., Rojas, M. I., Netto Flores Cruz, G., Hung, S. H., Rohwer, F., & Barr, J. J. (2016). Phage on tap-a quick and efficient protocol for the preparation of bacteriophage laboratory stocks. *PeerJ, 4*. https://doi.org/10.7717/peerj.2261. Article e2261.

Buonanno, M., Welch, D., Shuryak, I., & Brenner, D. J. (2020). Far-UVC light (222 nm) efficiently and safely inactivates airborne human coronaviruses. *Scientific Reports, 10*(1). https://doi.org/10.1038/s41598-020-67211-2. Article 10285.

Chiappa, F., Frascella, B., Vigezzi, G. P., Moro, M., Diamanti, L., Gentile, L., Lago, P., Clementi, N., Signorelli, C., Mancini, N., & Odone, A. (2021). The efficacy of ultraviolet light-emitting technology against coronaviruses: A systematic review. *Journal of Hospital Infection, 114*, 63–78. https://doi.org/10.1016/j.jhin.2021.05.005

Cutler, T. D., & Zimmerman, J. J. (2011). Ultraviolet irradiation and the mechanisms underlying its inactivation of infectious agents. *Animal Health Research Reviews, 12*(1), 15–23. https://doi.org/10.1017/S1466252311000016

van Doremalen, N., Bushmaker, T., Morris, D. H., Holbrook, M. G., Gamble, A., Williamson, B. N., Tamin, A., Harcourt, J. L., Thornburg, N. J., Gerber, S. I., Lloyd-Smith, J. O., de Wit, E., & Munster, V. J. (2020). Aerosol and surface stability of SARS-CoV-2 as compared with SARS-CoV-1. *New England Journal of Medicine, 382*(16), 1564–1567. https://doi.org/10.1056/NEJMc2004973

Eischeid, A. C., & Linden, K. G. (2011). Molecular indications of protein damage in adenoviruses after UV disinfection. *Applied and Environmental Microbiology, 77*(3), 1145–1147. https://doi.org/10.1128/AEM.00403-10

Elias, B., & Bar-Yam, Y. (2020). Could air filtration reduce COVID-19 severity and spread? New England complex systems Institute. Retrieved from https://necsi.edu/could-air-filtration-reduce-covid19-severity-and-spread. (Accessed 11 August 2021).

Gerchman, Y., Cohen-Yaniv, V., Betzalel, Y., Yagur-Kroll, S., Belkin, S., & Mamane, H. (2019). The involvement of superoxide radicals in medium pressure UV derived inactivation. *Water Research, 161*, 119–125. https://doi.org/10.1016/j.watres.2019.05.084

Gerchman, Y., Mamane, H., Friedman, N., & Mandelboim, M. (2020). UV-LED disinfection of coronavirus: Wavelength effect. *Journal of Photochemistry and Photobiology B: Biology, 212*. https://doi.org/10.1016/j.jphotobiol.2020.112044. Article 112044.

Greenhalgh, T., Jimenez, J. L., Prather, K. A., Tufekci, Z., Fisman, D., & Schooley, R. (2021). Ten scientific reasons in support of airborne transmission of SARS-CoV-2. *Lancet (London, England), 397*(10285), 1603–1605. https://doi.org/10.1016/S0140-6736(21)00869-2

Huang, C., Wang, Y., Li, X., Ren, L., Zhao, J., Hu, Y., Zhang, L., Fan, G., Xu, J., Gu, X., Cheng, Z., Yu, T., Xia, J., Wei, Y., Wu, W., Xie, X., Yin, W., Li, H., Liu, M., Xiao, Y., & Cao, B. (2020). Clinical features of patients infected with 2019 novel coronavirus in Wuhan, China. *Lancet (London, England), 395*(10223), 497–506. https://doi.org/10.1016/S0140-6736(20)30183-5

Inagaki, H., Saito, A., Sugiyama, H., Okabayashi, T., & Fujimoto, S. (2020). Rapid inactivation of SARS-CoV-2 with deep-UV LED irradiation. *Emerging Microbes & Infections, 9*(1), 1744–1747. https://doi.org/10.1080/22221751.2020.1796529

Janecek, M. (2012). Reflectivity spectra for commonly used reflectors. *IEEE Transactions on Nuclear Science, 59*, 490–497. https://doi.org/10.1109/TNS.2012.2183385

Jensen, M. M. (1964). Inactivation of airborne viruses by ultraviolet irradiation. *Applied Microbiology, 12*, 418–420. https://doi.org/10.1128/am.12.5.418-420.1964

Jensen, M. M. (1967). Bacteriophage aerosol challenge of installed air contamination control systems. *Applied Microbiology, 15*, 1447–1449. https://doi.org/10.1128/am.15.6.1447-1449.1967

Jones, B., Sharpe, P., Iddon, C., Hathway, E. A., Noakes, C. J., & Fitzgerald, S. (2021). Modelling uncertainty in the relative risk of exposure to the SARS-CoV-2 virus by airborne aerosol transmission in well mixed indoor air. *Building and Environment, 191*. https://doi.org/10.1016/j.buildenv.2021.107617. Article 107617.

Kowalski, W. (2009). *UV rate constants. Ultraviolet germicidal irradiation handbook*. Berlin, Heidelberg: Springer. https://doi.org/10.1007/978-3-642-01999-9_4

Lewis, D. (2021). COVID-19 rarely spreads through surfaces. So why are we still deep cleaning? *Nature, 590*(7844), 26–28. https://doi.org/10.1038/d41586-021-00251-4

Lombini, M., Diolaiti, E., De Rosa, A., Lessio, L., Pareschi, G., Bianco, A., Cortecchia, F., Fiorini, M., Fiorini, G., Malaguti, G., & Zanutta, A. (2021). Design of optical cavity for air sanification through ultraviolet germicidal irradiation. *Optics Express, 29*(12), 18688–18704. https://doi.org/10.1364/OE.422437

McDevitt, J. J., Rudnick, S. N., & Radonovich, L. J. (2012). Aerosol susceptibility of influenza virus to UV-C light. *Applied and Environmental Microbiology, 78*. https://doi.org/10.1128/AEM.06960-11. Article 1666.

Mebus, C. A., White, R. G., Stair, E. L., Rhodes, M. B., & Twiehaus, M. J. (1972). Neonatal calf diarrhea: Results of a field trial using a reo-like virus vaccine. *Veterinary Medicine, Small Animal Clinician, 67*(2), 173–174.

Megahed, N. A., & Ghoneim, E. M. (2020). Antivirus-built environment: Lessons learned from COVID-19 pandemic. *Sustainable Cities and Society, 61*. https://doi.org/10.1016/j.scs.2020.102350. Article 102350.

Melikov, A. K., Ai, Z. T., & Markov, D. G. (2020). Intermittent occupancy combined with ventilation: An efficient strategy for the reduction of airborne transmission indoors. *The Science of the Total Environment, 744*. https://doi.org/10.1016/j.scitotenv.2020.140908. Article 140908.

Missiakas, D. M., & Schneewind, O. (2013). Growth and laboratory maintenance of Staphylococcus aureus. *Current Protocols in Microbiology*. https://doi.org/10.1002/9780471729259.mc09c01s28 *(Chapter 9)*, Unit–9C.1.

Mittal, R., Ni, R., & Seo, J. (2020). The flow physics of COVID-19. *Journal of Fluid Mechanics, 894*, F2. https://doi.org/10.1017/jfm.2020.330

Morawska, L., Tang, J. W., Bahnfleth, W., Bluyssen, P. M., Boerstra, A., Buonanno, G., Cao, J., Dancer, S., Floto, A., Franchimon, F., Haworth, C., Hogeling, J., Isaxon, C., Jimenez, J. L., Kurnitski, J., Li, Y., Loomans, M., Marks, G., Marr, L. C., Mazzarella, L., & Yao, M. (2020). How can airborne transmission of COVID-19 indoors be minimised? *Environment International, 142*. https://doi.org/10.1016/j.envint.2020.105832. Article 105832.

Nannu Shankar, S., Witanachchi, C. T., Morea, A. F., Lednicky, J. A., Loeb, J. C., Alam, M. M., Fan, Z. H., Eiguren-Fernandez, A., & Wu, C. Y. (2022). SARS-CoV-2 in residential rooms of two self-isolating persons with COVID-19. *Journal of Aerosol Science, 159*. https://doi.org/10.1016/j.jaerosci.2021.105870. Article 105870.

Nardell, E. A. (2021). Air disinfection for airborne infection control with a focus on COVID-19: Why germicidal UV is essential. *Photochemistry and Photobiology, 97*(3), 493–497. https://doi.org/10.1111/php.13421

Ng, T. F., Kondov, N. O., Deng, X., Van Eenennaam, A., Neibergs, H. L., & Delwart, E. (2015). A metagenomics and case-control study to identify viruses associated with bovine respiratory disease. *Journal of Virology, 89*(10), 5340–5349. https://doi.org/10.1128/JVI.00064-15

Porex Filtration Group. (2021). *UV reflective media resources*. Retrieved from https://learn.porex.com/l/reflective-media. (Accessed 1 October 2021).

Qiao, Y., Yang, M., Marabella, I. A., McGee, D. A. J., Aboubakr, H., Goyal, S., Hogan, C. J., Olson, B. A., & Torremorell, M. (2021). Greater than 3-log reduction in viable coronavirus aerosol concentration in ducted ultraviolet-c (UV-C) systems. *Environmental Science & Technology, 55*, 4174–4182. https://doi.org/10.1021/acs.est.0c05763

Quill, T., Weiss, S., Hirschler, C., Pankadzh, V., Di Battista, G., Arthur, M., & Chen, J. (2016). Ultraviolet reflectance of microporous PTFE. *Proceedings of Porex Corporation, 4*, 1–12. Retrieved from https://www.porex.com/wp-content/uploads/2020/04/Ultraviolet-Reflectance-of-Microporous-PTFE.pdf. (Accessed 1 October 2021).

Rastogi, R. P., Richa Kumar, A., Tyagi, M. B., & Sinha, R. P. (2010). Molecular mechanisms of ultraviolet radiation-induced DNA damage and repair. *Journal of Nucleic Acids*. https://doi.org/10.4061/2010/592980, 2010 Article 592980.

Reed, N. G. (2010). The history of ultraviolet germicidal irradiation for air disinfection. *Public Health Reports, 125*, 15–27. https://doi.org/10.1177/003335491012500105

Retamar, M. E. M., Passalía, C., Brandi, R. J., & Labas, M. D. (2019). Dose estimation methodology for the UV inactivation of bioaerosols in a continuous-flow reactor. *Aerosol Science and Technology, 53*, 8–20. https://doi.org/10.1080/02786826.2018.1533914

Ryan, K., McCabe, K., Clements, N., Hernandez, M., & Miller, S. L. (2010). Inactivation of airborne microorganisms using novel ultraviolet radiation sources in reflective flow-through control devices. *Aerosol Science and Technology, 44*(7), 541–550. https://doi.org/10.1080/02786821003762411

SAGE. (2021). *Emg: Potential application of air cleaning devices and personal decontamination to manage transmission of COVID-19*. Retrieved from https://www.gov.uk/government/publications/emg-potential-application-of-air-cleaning-devices-and-personal-decontamination-to-manage-transmission-of-covid-19-4-november-2020. (Accessed 1 October 2021).

Shah, Y., Kurelek, J. W., Peterson, S. D., & Yarusevych, S. (2021). Experimental investigation of indoor aerosol dispersion and accumulation in the context of COVID-19: Effects of masks and ventilation. *Physics of Fluids, 33*(7). https://doi.org/10.1063/5.0057100. Article 073315.

de Sternberg Stojalowski, P., & Fairfoull, J. (2021). Comparison of reflective properties of materials exposed to ultraviolet-C radiation. *Journal of Research of the National Institute of Standards and Technology, 126*. https://doi.org/10.6028/jres.126.017. Article 126017.

Tang, J. W., Marr, L. C., Li, Y., & Dancer, S. J. (2021). COVID-19 has redefined airborne transmission. *BMJ, 373*. https://doi.org/10.1136/bmj.n913. Article n913.

Thatcher, C. H., & Adams, B. R. (2021). Impact of surface reflection on microbial inactivation in a UV led treatment duct. *Chemical Engineering Science, 230*. https://doi.org/10.1016/j.ces.2020.116204. Article 116204.

The Lancet. (2020). COVID-19: Protecting health-care workers. *Lancet (London, England), 395*(10228), 922. https://doi.org/10.1016/S0140-6736(20)30644-9

Tseng, C. C., & Li, C. S. (2005). Inactivation of virus-containing aerosols by ultraviolet germicidal irradiation. *Aerosol Science and Technology, 39*(12), 1136–1142. https://doi.org/10.1080/02786820500428575

Turgeon, N., Toulouse, M. J., Martel, B., Moineau, S., & Duchaine, C. (2014). Comparison of five bacteriophages as models for viral aerosol studies. *Applied and Environmental Microbiology, 80*(14), 4242–4250. https://doi.org/10.1128/AEM.00767-14

Walker, C. M., & Ko, G. (2007). Effect of ultraviolet germicidal irradiation on viral aerosols. *Environmental Science & Technology, 41*(15), 5460–5465. https://doi.org/10.1021/es070056u

World Health Organisation (WHO). (2021). *Roadmap to improve and ensure good indoor ventilation in the context of COVID-19*, ISBN 9789240021280. Retrieved from https://www.who.int/publications/i/item/9789240021280. (Accessed 11 August 2021).

Wu, D., Wu, T., Liu, Q., & Yang, Z. (2020). The SARS-CoV-2 outbreak: What we know. *International Journal of Infectious Diseases, 94*, 44–48. https://doi.org/10.1016/j.ijid.2020.03.004

Wu, F., Zhao, S., Yu, B., Chen, Y. M., Wang, W., Song, Z. G., Hu, Y., Tao, Z. W., Tian, J. H., Pei, Y. Y., Yuan, M. L., Zhang, Y. L., Dai, F. H., Liu, Y., Wang, Q. M., Zheng, J. J., Xu, L., Holmes, E. C., & Zhang, Y. Z. (2020). A new coronavirus associated with human respiratory disease in China. *Nature, 579*(7798), 265–269. https://doi.org/10.1038/s41586-020-2008-3

Zhang, Y., Mo, J., Li, Y., Sundell, J., Wargocki, P., Zhang, J., Little, J. C., Corsi, R., Deng, Q., Leung, M., Fang, L., Chen, W., Li, J., & Sun, Y. (2011). Can commonly-used fan-driven air cleaning technologies improve indoor air quality? A literature review. *Atmospheric Environment, 45*(26), 4329–4343. https://doi.org/10.1016/j.atmosenv.2011.05.041

Zhou, L., Yao, M., Zhang, X., Hu, B., Li, X., Chen, H., Zhang, L., Liu, Y., Du, M., Sun, B., Jiang, Y., Zhou, K., Hong, J., Yu, N., Ding, Z., Xu, Y., Hu, M., Morawska, L., Grinshpun, S. A., Biswas, P., & Zhang, Y. (2021). Breath-, air- and surface-borne SARS-CoV-2 in hospitals. *Journal of Aerosol Science, 152*. https://doi.org/10.1016/j.jaerosci.2020.105693. Article 105693.